




Concise Historic Overview of Rail Corrugation Studies: From Formation Mechanisms to Detection Methods

Qi-Ang Wang ^{1,*} , Xin-Yu Huang ¹, Jun-Fang Wang ^{2,*} , Yi-Qing Ni ³ , Sheng-Cai Ran ⁴, Jian-Peng Li ¹ and Jia Zhang ¹

¹ State Key Laboratory of Geomechanics and Deep Underground Engineering, School of Mechanics and Civil Engineering, China University of Mining and Technology, Xuzhou 221116, China

² National Key Laboratory of Long-Life Road Engineering in Extreme Environment, College of Civil and Transportation Engineering, Shenzhen University, Shenzhen 518060, China

³ National Rail Transit Electrification and Automation Engineering Technology Research Center (Hong Kong Branch), Department of Civil and Environmental Engineering, The Hong Kong Polytechnic University, Hong Kong, China

⁴ College of Urban Construction, Heze University, Heze 274021, China

* Correspondence: qawang@mail.nwpu.edu.cn (Q.-A.W.); jf.wang@szu.edu.cn (J.-F.W.)

Abstract: Rail corrugation is a serious problem in a railway transportation system, aggravating the operational risk and shortening the lifetime of train–track system. In order to ensure the safety and reliability of the railway system, the detection of rail corrugation is very important. Thus, this study systematically summarizes the recent research progress of rail corrugation. First, this study introduces the definition of rail corrugation and the classification criteria. Then, the formation mechanism of rail corrugation is analyzed in detail, and its adverse consequences are investigated. Further, this study summarizes several main detection methods, which are corrugation-detection methods based on acceleration measurements, wavelet transform methods for corrugation evaluation, computer-vision-based methods for corrugation automatic detection, digital filtering algorithms for rail corrugation detection, and others. In this study, the formation mechanism and detection methods of rail corrugation are systematically described, and various corrugation-detection methods are also introduced in detail. This study not only provides a scientific basis for railway maintenance, but also lays a solid foundation for future experimental design and data analysis. This study can also guide engineering practice to improve the reliability and safety of railway systems. It also provides useful experience for future railway-engineering design and planning, as well as safer and more reliable operation. In general, this study can provide technical support for the detection of rail corrugation to ensure the safety of the rail–track system.

Keywords: rail corrugation; corrugation formation mechanism; detection method; structural health monitoring; wheel–rail interface



Citation: Wang, Q.-A.; Huang, X.-Y.; Wang, J.-F.; Ni, Y.-Q.; Ran, S.-C.; Li, J.-P.; Zhang, J. Concise Historic Overview of Rail Corrugation Studies: From Formation Mechanisms to Detection Methods. *Buildings* **2024**, *14*, 968. <https://doi.org/10.3390/buildings14040968>

Academic Editors: Maxim A. Dulebenets, Osama Abudayyeh and Xinzhuang Cui

Received: 5 December 2023

Revised: 11 March 2024

Accepted: 25 March 2024

Published: 1 April 2024



Copyright: © 2024 by the authors. Licensee MDPI, Basel, Switzerland. This article is an open access article distributed under the terms and conditions of the Creative Commons Attribution (CC BY) license (<https://creativecommons.org/licenses/by/4.0/>).

1. Introduction

Rail transit is one of the most crucial means of transport in the world due to its advantages, including low cost, large volume of transport, punctuality, safety, and high reliability. In the current, increasingly interconnected, world, rail transport plays an irreplaceable role as a sustainable and efficient mode of transport. With the continuous expansion of global trade and the rapid development of urbanization, the demand for railway transportation is also gradually increasing. Railways are not only a link between cities and countries but also an important cornerstone for economic prosperity and social stability. Its characteristics of low carbon, high efficiency, and large capacity make it a sustainable transportation backbone, and at the same time, it is also a key component in promoting the smooth flow of global supply chains. Rail transport is an important part of the economic development of many countries, and statistics show that there has been a huge growth in the global

rail network over the past 20 years [1–3]. The implementation of new technologies and better infrastructure will provide a much-needed boost to the rail transport sector. In some countries of the European Union, expenditure on rail transport is several times that of road transport [4,5]. For the past decades, China's high-speed railway has developed quickly; the length of the high-speed rail has reached 40,000 km and formed a relatively complete transportation system. As one of the crucial parts of the rail system, the rail carries all the loads of the train. Rail damage to steel is usually caused by the dynamic wheel–rail contact, which leads to the shortening of the safe service life of the rail system, and is very detrimental to the safety, comfort, and reliability of rail transit. Therefore, the control of rail damage is very important to the safety and comfort of vehicle operation.

As a result of the vibration and wheel–rail impact, when the training mileage reaches a certain degree, the rail surface will form a variety of damage defects, including uneven rail welding, ballast track imprint, rail collapse, longitudinal deformation, rail transverse section deformation, and surface-fatigue deformation. As a common rail damage, rail corrugation has complex mechanisms and difficult treatment. Rail corrugation, also known as rail-surface corrugation, is a kind of rail surface along the longitudinal corrugation phenomenon. Its wavelength distribution is 20–1200 mm, and the excitation frequency is 30–2000 Hz. The vibration and noise induced by rail corrugation not only affect the passenger's ride comfort but also aggravate the fatigue damage of the vehicle and track components, endangering the safety of the railroad. According to statistics, nearly 40% of the orbits in the world produce corrugation hazards.

The research into rail corrugation is a gradual process. In 1889, world railway experts carried out research activities on the rail corrugation phenomenon on the Midland line in Britain but failed to give a reasonable explanation for its formation mechanism. Since 1895, the same problem has also existed in Britain, Canada, Germany, Japan, Australia, and other countries, for which Sato et al. [6] made a relatively comprehensive review of the aspects of rail mill initiation, classification, and suppression.

As one of the unavoidable problems in the world of railway technology and theoretical research, rail corrugation is still a major technical problem to be further worked out in the railway industry. At present, there are many comprehensive reports on rail corrugation in China and abroad [6–12]. People have a deepening understanding of the manifestations and formation mechanism of rail corrugation and have formed classification methods with their characteristics. Jin et al. [13] comprehensively summarized and prospected the generation mechanism and suppression methods of rail corrugation in the past 40 years. Moreover, Grassie et al. [9] proposed two kinds of formation mechanisms for rail corrugation, i.e., a wavelength-fixing mechanism and a damage mechanism, and divided rail corrugation into six categories [12]. For rail corrugation-monitoring techniques, there exist different kinds of methods, including Fiber Bragg Grating (FBG), the acoustic emission technique, piezoelectric sensor, radio-frequency identification (RFID) technique [14,15], etc.

In summary, rail corrugations can accelerate the wear of rails, wheels, and other equipment, reduce the service life of rail systems, and increase the resistance of the train during the running process, affecting the efficiency of railway transportation. Also, rail corrugations can generate noise pollution. Therefore, the purpose of this study is to carry out a systematic review of the formation mechanism and detection methods of rail corrugations, so as to reduce the harm of rail corrugations.

In this study, the characteristics of rail corrugation are comprehensively analyzed, the typical characteristics are summarized, the definition of rail corrugation is provided, and the classification methods, formation mechanism, damage and detection methods of rail corrugation are summarized to provide reference and guidance for research into the formation mechanism and detection methods of rail corrugation.

2. Definition and Classification of Rail Corrugation

2.1. Rail-Corrugation Definition

Rail corrugation refers to the periodic wave wear along the longitudinal surface of the rail, and it has two properties: wavelength and peak valley. The periodic wave wear not only makes the rail surface gradually form regular corrugations but also presents a certain friction and wear difference between the peak and trough of the rail corrugation. Such features are complex and diverse, involving the comprehensive influence of track structure, material properties, and other factors. In Figure 1, the obvious wave wear formed along the longitudinal surface of the rail can be clearly observed. These corrugations show a regular periodic arrangement in the orbit and extend far away. The corrugation peaks and troughs are clearly visible and constitute the basic morphology of the rail-corrugation phenomenon. The causes of rail corrugation are complex and have various manifestations. Therefore, rail corrugation has different classification standards. In this study, the following classification criteria are presented: corrugation classification by wavelength, wavelength determination mechanism and rail damage mechanism, and rail wear type.



Figure 1. Schematic diagram of rail corrugation.

2.2. Rail-Corrugation Classification by Wavelength

Rail corrugation can be divided into the short-wavelength corrugation and the long-wavelength corrugation according to the wavelength. The short wavelength is between 30 mm and 80 mm, and the wave depth is between 0.1 mm and 0.5 mm. The short-wavelength corrugation often occurs on high-speed linear lines with lighter axle loads [16], and it can often be detected on the curved inner rail surface. It is one of the most common types of rail corrugation [7].

The long-wavelength corrugation is also called the wave-type corrugation. Its wavelength is greater than 100 mm, and the wave depth is often below 2 mm. Long-wavelength corrugation is common on the surface of the outer rail, which has a heavy load and a small radius curve. The peaks and troughs of the wave are uniform in gloss, and the plastic deformation of the rail surface is more prominent at the troughs.

2.3. Rail-Corrugation Classification by Wavelength Determination Mechanism and Rail Damage Mechanism

According to the determination mechanism and rail damage mechanism, rail corrugations can be roughly divided into heavy-duty rail corrugation, light rail corrugation, elastic sleeper corrugation, contact-fatigue corrugation, rut corrugation, and sound rail corrugation [17]. The specific classification is shown in Table 1. Type 1 is heavy-duty rail corrugation. Type 2 is light rail corrugation. Type 3 is elastic sleeper rail corrugation. Type 4 is contact fatigue rail corrugation. Type 5 is rut rail corrugation. Type 6 is sound rail corrugation.

Table 1. Classification of rail corrugation [12].

Types	Frequency	Wavelength Determination Mechanism	Loss Mechanism	Location
Type 1	50–100 Hz	P2 force resonance frequency for vertical vibration	Plastic deformation at the trough	Straight line, curved line
Type 2	50–100 Hz	P2 force resonance frequency for vertical vibration	Plastic bending of rails	Straight line, curved line
Type 3	140–280 Hz	Ill-conditioned elastic sleeper resonance frequency	The initial stage is dominated by wear, and after corrugation, plastic flow is dominated	Straight line, curved line
Type 4	150–450 Hz	Wheel–rail surface contact fatigue caused by P2 force	Rolling contact fatigue	Straight line, curved line
Type 5	250–400 Hz	Wheelset torsional resonance, maximum vertical contact load between wheel and rail	Wave trough longitudinal vibration wear	Curved line
Type 6	400–1200 Hz	Unknown	Longitudinal sliding wear of wave trough	Straight line, curved line

2.4. Rail-Corrugation Classification by Rail Wear Type

According to whether the rail head is worn or plastically deformed, referring to the appearance characteristics of the rail corrugation on site, corrugations can be divided into three categories: abrasion corrugation, plastic-flow corrugation, and hybrid corrugation.

Abrasion corrugation mainly results from uneven wear in the area of railheads. The abrasion corrugation mainly appears on harder rails such as quenched rails. The surface wear marks are obvious, and the color of the wave peaks and peaks and valleys is consistent. The longitudinal profile of the corrugated rail is completely similar, and the rail head of the worn corrugated rail is smooth.

Plastic-flow corrugation mainly results from uneven plastic deformation of the rail head. It is more common on heavy-duty roads. It is formed by plastic deformation of the rail surface due to excessive vertical load. Under heavy loads, the trough is often accompanied by significant plastic deformation.

Hybrid corrugation is generally caused by uneven wear and uneven plastic deformation, which combines the comprehensive characteristics of wear and plastic-flow corrugation.

3. Formation Mechanisms of Rail Corrugation

3.1. Formation Mechanisms

Generally, there are mainly three types of formation mechanisms for rail corrugation [18]. (a) Regarding a sharp curve, the length between the inside and outside of the rail is different. This difference cannot be absorbed by the difference in the rolling radius of the wheel. In this case, the longitudinal creep force is generated between the rail and the wheel. This creep force will force the axle to twist, which will cause the rail corrugation. (b) Rail corrugation can also be induced by the periodic wear caused by stick–slip oscillation. (c) The rail irregularity will generate a large wheelset vibration, which will induce the rail corrugation.

Matsumoto et al. [18] established a mathematical model to explain the formation mechanism of corrugation through experimental tests. The relative position of the bogie and track in curving is mastered by creating non-contact measurement methods. Liu and Wang [19] developed a model of torsional vibration in the time domain to explain the reason why most corrugations occur on the inner rail. The model also proves that the torsional vibration amplitude increases with the curvature of the rail. What is more, Suda et al. [20] analyzed the measured experimental data in detail through wavelet analysis and concluded that the development mechanism of rail corrugation is caused by the following reasons. (a) Steady-state longitudinal slip is a critical influence factor, that will determine

the type and wavelength of corrugation, the wear rate of rails, and the developing process of corrugations. (b) Rails will form short-pitch corrugation in the condition of low creepage. (c) If the slip condition is relatively large, long-wavelength corrugation will appear. (d) The formation mechanism of corrugations is related to the wear rate and can also be explained by the phase relation between the corrugation profile, contact load, and slip. The physical drawing of the corrugation simulator and outline of the corrugation simulator are shown in Figure 2.

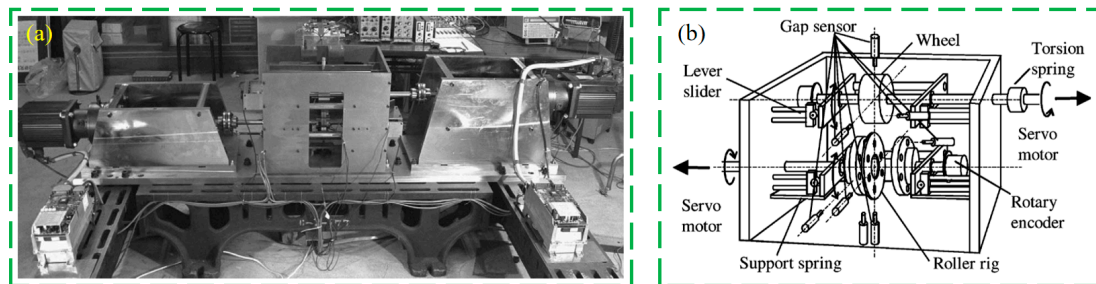


Figure 2. (a) Physical drawing of corrugation simulator; (b) construction diagram of corrugation simulator [20].

In terms of other research methods, Wang and Lei [21] used the three-dimensional finite-element model of a wheel–rail system to carry out the complex eigenvalue analysis of influence factors for corrugation. In this study, it is found that in order to increase the stability of the wheel–rail system and suppress its unstable vibration, it is necessary to maintain the balanced superelevation of the track structure, which can play a critical role in suppressing the corrugation of the rail. Unstable friction self-excites vibration of the wheel–rail system and generally results from the excess and deficient superelevation states of the track structure. The former appears in the inner wheel–inner rail and the latter in the outer wheel–outer rail. That is the reason why only one side of the rail is corrugated. Figure 3 shows the frictional self-excited vibration model of the wheel–rail system and the wheel–rail contact geometry relationship. The model consists of a wheelset, two rails, and a flat plate. A spring–damping element is used to simulate the fastener to realize the connection between the rail and the slab.

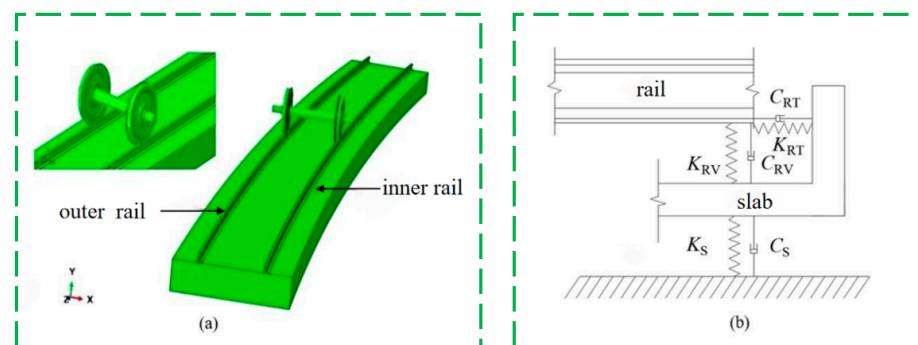


Figure 3. (a) Configuration of wheel–rail system; (b) geometric relationship diagram of rail and slab [21].

Wang and Lei [22] also studied the stick–slip characteristics of wheel–rail contact under different super, standard, and high conditions and found that both the inner and outer wheel–rail systems had the possibility of a stick–slip movement on the small-radius curve of the subway, and the inner wheel–rail system was more likely to cause the formation of rail corrugation.

In addition to the aforementioned study, Du et al. [23] studied the influence of grinding on the development of rail corrugation and tested the vibration characteristics of grinding systems through simulation models and force hammer tests. The following conclusions

are drawn: (a) when the grinding train is running at 12~13 km/h, the surface of the rail will produce wear marks with a wavelength of about 60 mm, and the marks are regular; (b) through the dynamic simulation model and the force hammer test, it is revealed that ground vibration will be caused when the grinding train runs at a frequency of 60 Hz; (c) by changing the grinding speed, the hydraulic system stiffness can be adjusted, and the interval of grinding marks will also be changed; (d) if the frequency of the wheel and rail excited by the grinding mark is the same as the pinned frequency of the rail, rail corrugation may occur.

Based on the mechanism of rail-corrugation formation summarized in the review literature, this study believes that wheel–rail interaction, hardness of rail material, track geometry, and train speed are interwoven to form a complex corrugation pattern.

3.2. Analysis of Influencing Factors Leading to Rail Corrugation

3.2.1. Effect of Uneven Velocity Distribution on the Growth of Corrugation in Curves

This section mainly introduces the influence of uneven velocity distribution (or asymmetry) on the waveform growth of bends. A waveform-growth prediction model, including quasi-static bogie turning dynamics, is established, and the waveform growth under the condition of non-uniform velocity distribution is studied [19].

Under typical cornering conditions, the corrugation growth rate increases (or decreases) when the mean or skewness of the distribution's passing speed set is biased toward higher (or lower) speeds. An uneven velocity distribution can result in a reduction of up to 50% in the predictive effectiveness of the expanded velocity distribution control to reduce the corrugation growth rate [24].

3.2.2. Influence of Wheel–Rail Contact Angle and Saturated Creep Force Direction on Rail Corrugation

The phenomenon of rail corrugation on tightly curved tracks is studied in this section. The stability of the wheel–rail system is studied by using the finite-element complex eigenvalue method, and the elastic vibration model of the front wheel–rail system is established [25].

The simulation results show that the saturated creep force will cause the self-excited vibration of the wheel–rail system and lead to rail wrinkling. The effects of contact angle and saturated creep force direction on the self-excited vibration of the front wheelset–crawler system are studied. The transverse saturated creep force produces rail corrugation more easily than the longitudinal saturated creep force [25]. The detailed layout of springs and dampers is shown in Figure 4.

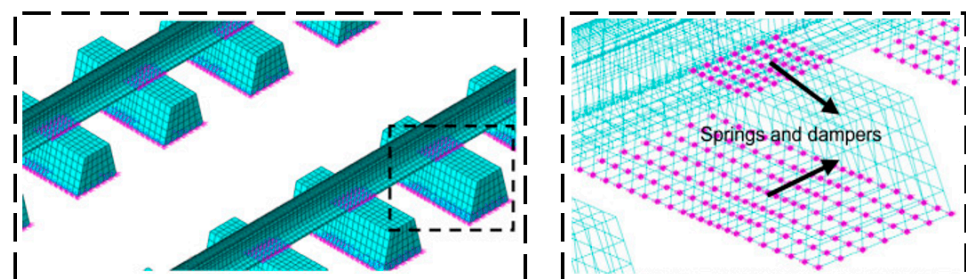


Figure 4. Detailed layout of springs and dampers [25].

3.2.3. Influence of Rolling Contact Fatigue on Rail Corrugation

Du et al. [23] analyzed the dynamic characteristics of rail-grinding trains through simulation models, tested the vibration characteristics of the grinding system, and studied the relationship between the grinding-operation process and the development of rail corrugation.

In this study, the maintenance and grinding effects of standard and heat-treated pearlite rails are studied experimentally. The results show that the behaviors of the two kinds of steel are essentially different. In the standard grade, in the process of use, the

friction-induced martensite (FIM) produced in the grinding process will change. However, grinding will cause serious surface deformation, which is consistent with the deformation caused by train operation, resulting in rail “pre-fatigue” [23].

3.2.4. Effect of Wheel–Rail Vibration on Rail Corrugation

Wang and Lei [21,26] used the three-dimensional finite-element model of a wheel–rail system to conduct the complex eigenvalue analysis on the influencing factors of rail corrugations. The stability of the wheel–rail system with different vertical and lateral stiffnesses of fasteners, different friction coefficients, and different track-structure superelevation was analyzed. To maintain the stability of the wheel–rail system, it is necessary to maintain the balanced superelevation of the track structure. This will inhibit the generation of rail corrugation.

This study mainly investigates the wheel–rail friction self-excitation and establishes the corresponding finite-element model of the wheel–rail system and rail wear surface with irregular waveform. Then, the response and stability of the wheel–rail system on smooth and worn surfaces can be studied by considering the influence of self-excited vibration of the wheel–rail friction and feedback vibration of ripple irregularity, and the power source of rail ripple is explored [27,28].

3.2.5. Influence of Sleeper Distance on Rail Corrugation

Ng et al. [29] modeled, analyzed, and predicted rail-corrugation growth under the influence of sleeper distance. The wheel–rail interaction model is established based on the three-dimensional finite-element method. The results show that a 700 mm sleeper distance produces a higher corrugation growth rate than a 500 mm sleeper distance. Therefore, a sleeper distance of 500 mm is recommended to reduce the growth of rail corrugation.

Ng and Martua [30] further modeled and predicted rail-corrugation growth for four different track configurations (different rail metallurgy, sleeper distance, and track system). Through 3D finite-element modeling and signal processing, the results showed that rail corrugation increases exponentially with time, with ballast track and head-hardening track with sleeper spacing of 700 mm showing the slowest corrugation growth.

Vadillo et al. [31] investigated the effect of sleeper separation on rail-corrugation growth. With an initial sleeper separation of 1000 mm, corrugation depths measured up to 0.42 mm peak to peak after the passing of only 920,000 wheelsets. With the insertion of intermediate sleepers, hence the reduction of separation to 500 mm, corrugation growth was found to cease.

3.3. Adverse Consequences Caused by Rail Corrugation

3.3.1. Damage to the Train

Rail corrugation is periodic wear along the longitudinal surface of the rail after repeated rolling by wheels [32] and has a relationship with the inherent characteristics of the vehicle track. Its formation and development process will lead to the reduction of train comfort, safety, and stability. By aggravating the vibration damage of vehicle track parts, in serious cases, it will lead to vibration fatigue damage or the fracture of some parts (such as fasteners, track plates, sleepers, frames, and axle boxes), affecting the safety of train operation.

The research shows that the corrugation of small-radius curve rail is common and harmful in heavy-haul railways. Its wavelength and wave depth are closely related to the action force between the wheel and rail [33]. The greater the wave depth and the shorter the wavelength, the greater the harm to the operational safety of the locomotive. Under the condition of high-speed driving, the harm of rail corrugation is much greater than that at low speed, and wheel–rail separation is very likely to occur, resulting in strong impact vibration.

3.3.2. Damage to the Track

There are many urban rail curves, various track types, and frequent acceleration and deceleration of vehicles, resulting in many rail corrugation diseases in the urban rail system. Its types and characteristics are different from large railways, with an early occurrence and rapid development rate, mainly short-wave grinding below 100 mm. Urban rail corrugation will cause a series of secondary diseases, such as fastener elastic strip fracture, fastener T-bolt fracture, abnormal noise in the vehicle, and so on. The secondary diseases caused by rail corrugation are shown in Figure 5.



Figure 5. Secondary diseases caused by rail corrugation [34].

The initiation of rail corrugation causes severe vibration of rolling stock and the track structure, which does serious harm to the track structure. The surface irregularity causes the sharp increase of the wheel–rail force, which greatly shortens the service life of relevant parts of the locomotive and vehicle and track structure. Furthermore, the rail corrugation is also prone to cause serious damage to the subgrade, resulting in an increase in the damage rate of various parts of the line, which greatly increases the relevant maintenance workload and maintenance cost of the public works department. Meanwhile, the vibration and noise generated by rail corrugation are prone to cause discomfort to passengers and seriously affect the train-riding environment. In addition, corrugation will also increase the running resistance of the train. If the disease is serious, under the influence of wheel–rail force, not only the track bed will be damaged but the axle and rail may also be broken, which will seriously endanger the safety of train operation [35]. Figure 6 shows rail damage on site.

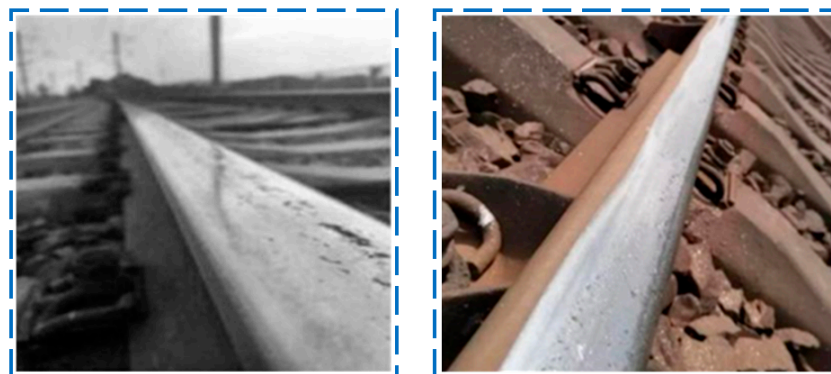


Figure 6. On-site rail damage [35].

The vibration and noise generated by the vehicle passing through the wave grinding track not only affect the passenger's riding comfort but also aggravate the fatigue damage of vehicle and track components and endanger driving safety. As shown in Figure 6, the fastener elastic strips at two adjacent places on the wave grinding track are broken.

3.3.3. Rail-Component Damage and Environmental Radiation Noise

The wear caused by rail corrugation not only accelerates the fatigue of the rail surface but may also initiate cracks and damage between the crest and trough, which gradually evolve into severe rail-component damage. This damage not only affects the structural integrity of the track but also poses a potential threat to the smoothness and safety of the train during running. In addition, rail corrugation is also closely linked to environmental radiation noise, becoming an important source of noise pollution in urban and rural areas. The vibration and noise caused by rail corrugation will not only negatively affect the quality of life of the surrounding residents but also may cause the environmental radiation noise to exceed the normal level and affect the nearby natural ecosystem.

With the large-scale construction of subways in various cities, they are also facing new problems, such as bolt fracture, elastic strip fracture, noise in the carriage, environmental radiation noise of the viaduct, and so on. These problems not only increase the maintenance cost of the track system but also affect the safe operation of trains. Figure 7 shows the cracked clips on the corrugated rail.

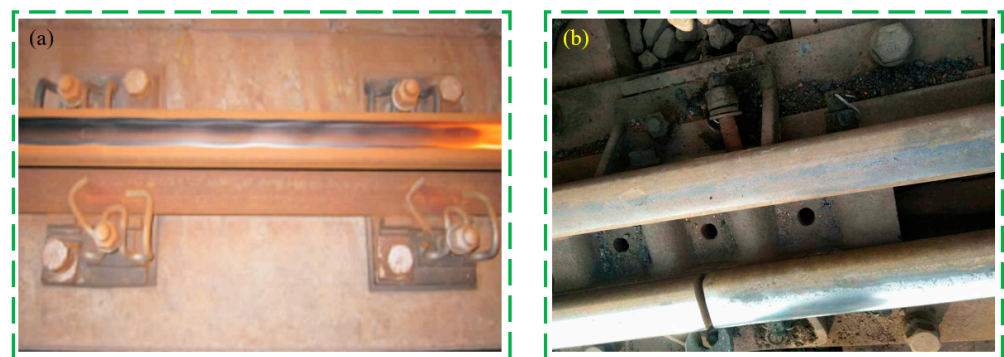


Figure 7. (a) Cracked clips on corrugated rail; (b) bolt fracture.

4. Detection Methods for Rail Corrugation

4.1. Corrugation Detection Based on Acceleration Measurements

At present, there is much research on rail-corrugation detection on the basis of acceleration-response analysis. Huang et al. [36] proposed a new detection technique for rail corrugation and this technique is based on a fiber laser accelerometer. In order to estimate the rail corrugations accurately, the principle and algorithm of double integral and wavelet denoising were proposed. Li et al. [37–40] proposed a new wavelength estimation method based on wheel-vibration acceleration. Ensemble empirical mode decomposition (EEMD) was used to estimate the wavelength, and a support-vector machine (SVM) was used to extract double chest features for depth recognition. Li et al. [41] also designed a vehicle–rail vertical coupling system and employed the empirical mode decomposition method and bispectrum analysis to obtain rail-corrugation features on the basis of wheelset vibration signals. The detection accuracy of normal rail corrugation based on the proposed algorithm can be up to 100%, and the classification accuracy can be up to 99% under the corrugation depths of 0 mm, 0.01~0.03 mm, 0.04~0.07 mm, and 0.08~0.1 mm. In addition, corresponding research is also carried out for the different sensor locations. Wei et al. [42–45] conducted simulation experiments for corrugation detections using bogie frame accelerations. Tanaka et al. [46] measured the track surface roughness on the basis of axle box accelerations. It is concluded that rail surface roughness is closely related to axle box accelerations. The appearance of the trolley and sensor arrangement is shown in Figure 8. The trolley can continuously measure the surface roughness of the rail on the side of the sensor unit by manually pushing on the track. Moreover, many corrugation-detection studies are conducted based on the wheel-bearing vibration data. Alten et al. [47] carried out the research on the basis of wheel-bearing vibration. Rail corrugations can be automatically detected and classified by training a classifier for a series of vibration features.

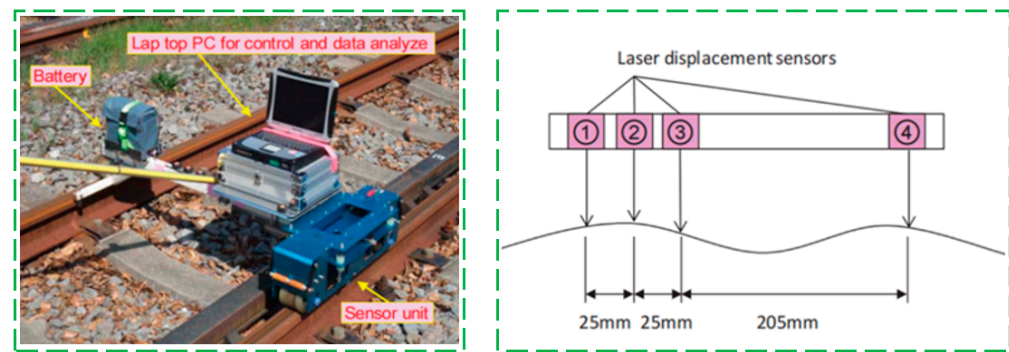


Figure 8. Continuous-measuring trolley and sensor arrangement [46].

In addition to previous methods, Grassie et al. [48] used the machine-learning algorithm to test the acceleration response characteristics, applied the machine-learning method to the vehicle data of the urban rail department, and used the vibration data to evaluate the status of the rail head. In order to better simulate the real state, the vibration signal used comes from the detection of the front axle bearing of the unpowered bogie. At the same time, the regression model was used to compensate for and eliminate the influence of vehicles, and the expected amplitude of each feature of each box was obtained at the current speed. There are also studies on the classification of the rail-corrugation degree of the Vienna tramcar track, using a regression model to compensate, and using a machine-learning algorithm to test vibration acceleration characteristics, to eliminate the effect of rail corrugation on vehicles [49].

4.2. Wavelet Transform Methods for Corrugation Evaluation

In order to better detect rail corrugation, relevant scholars have carried out research on the wavelet transform method. Dong et al. [50–53] investigated the rail-corrugation fault-detection method based on wavelet packet energy entropy, established the model by using a multi-body dynamics software, calculated the wavelet packet energy entropy and the wavelet energy of each node, and judged the rail-corrugation situation. The simulation results show that wavelet packet energy entropy can judge the condition of rail corrugation well. In addition, Liu et al. [54] proposed an indirect method based on wavelet packet decomposition and wheel–rail noise levels to evaluate corrugation amplitudes at different wavelengths. The effectiveness of the proposed method was verified by direct measurement, and the average error of the estimated amplitude was 10.5%.

However, for other detection methods, Taheri et al. [55] investigated a more advanced sensory system, and a signal-processing algorithm was developed to detect various irregularities on the track surface. The train dynamics caused by rail defects were simulated by using the wheel–rail dynamics model, and the potential of the new technology in rail defect detection was evaluated. In the meantime, the algorithm proposed by Taheri et al. [56] uses continuous and discrete differential wavelet filters to process data, locate defects, and provide information that distinguishes rail types and wheel defects, including rail cracks, squatting, and wave grinding. The wavelet algorithm is applied to the sampling signal of the accelerometer, and the results show that the algorithm has the potential to locate and diagnose the defect of the bogie with limited vertical acceleration.

4.3. Computer-Vision-Based Methods for Corrugation Automatic Detection

Computer-vision-based monitoring methods are also frequently used in corrugation detection. Li et al. [57] introduced an efficient visual detection system for rail corrugation, which can extract the frequency feature vectors of each column of the track image and determine whether the column is a corrugation line based on a support-vector machine (SVM). The experiment results show the precision and recall of the proposed corrugation-detection system are 98.47% and 96.50%, respectively. The system is shown in Figure 9. On this basis, Li [58] and his team carried out further research. They statistically analyzed the

Fourier transform coefficients of rail corrugation lines and background lines in rail images. It is found that the energy of the corrugated lines is more concentrated, while the energy of the background lines is more dispersed. A rail-corrugation-detection method based on rail image frequency domain features is proposed. The results show that the precision rate and recall rate of the proposed method is 92. They [59] also segmented the track image with the machine-learning algorithm and recognized it as SVM.

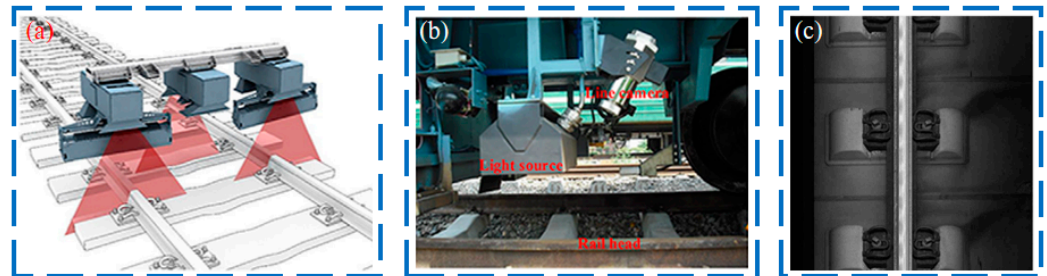


Figure 9. Configuration of image-acquisition subsystem. (a) the schematic diagram of image acquisition; (b) the real scene picture of this subsystem; (c) an example of track images captured by this system [57].

Similarly, Wei et al. [60] also converted the rail-corrugation recognition problem into an image-classification problem and used the classifier to determine whether the rail image is a corrugation rail image or not. An improved Spatial Pyramid Matching model based on integrating multi-features and locality-constrained linear coding is proposed. The quantitative experiment results demonstrate that the proposed corrugation identification method can achieve a higher precision rate and recall rate than those of traditional methods, reaching 99.67% and 98.34%, respectively. Figure 10 illustrates the process diagram of the rail-surface localization method. Aiming to solve the problem that the rail surface is not sensitive to lighting and reflection characteristics, Chen et al. [61] proposed a bi-linear laser-assisted method. This method can locate the railhead boundary and measure the position deviations of the rail corrugation measuring point based on the string, and no additional light source is required. The experiment results show that the accuracy of the position deviation of the chord-based measuring points is limited to within 0.4 mm.

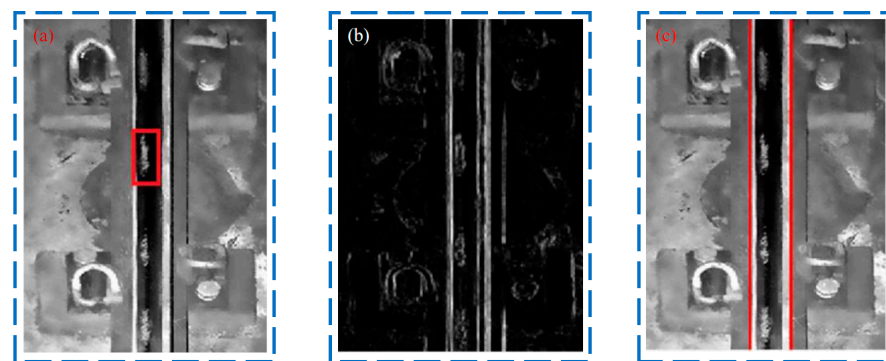


Figure 10. Rail-surface localization procedure. (a) original image before localization; (b) vertical edge enhancement results; (c) image results after localization [60].

In addition, other scholars have also carried out a lot of research on the detection method of computer vision. Wang and Zeng [62] rectified the corrugation measuring points on the center line of the deviating track head and optimized the inverse filter parameters to achieve perfect waveform recovery. Figure 11 shows the ideal measuring points and deviated measuring points. This method can be used for broadband measurement on rail corrugation effectively. The geometry of the three-line structured-light vision model is also shown in Figure 11. Three parallel light planes intersect with the rail to form three laser stripes of the rail profile, respectively. For other rail-corrugation-detection methods,

Mmg et al. [63] proposed a machine-vision-based corrugation measurement system for rail damage evaluation. The system uses a robust laser peak detection algorithm with sub-pixel accuracy to measure the amplitude of rail corrugation with an accuracy of up to 4 microns. It is worth mentioning that Yang et al. [64] proposed a real-time detection method for rail corrugation based on machine vision and a convolutional neural network. According to the gray characteristics of each part of the image, a method of rail-surface segmentation based on the maximum gray value of the sliding window is proposed. The image of the rail surface obtained by this method is clearer, and the characteristic information of the rail surface can be completely preserved.

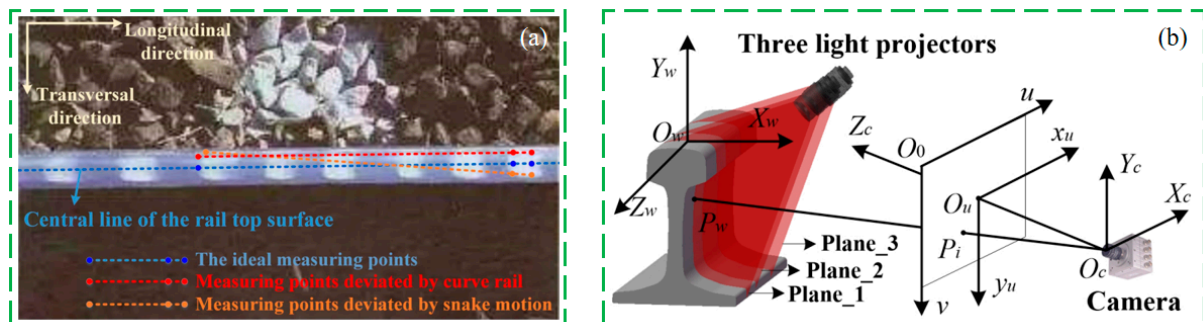


Figure 11. (a) Ideal measuring point and deviation measuring point; (b) schematics of the triple-line structured-light vision model [62].

4.4. Digital Filtering Algorithms for Rail-Corrugation Detection

Digital filtering algorithms are also widely used to detect rail corrugation. Mandriota et al. [65] proposed a fast rail corrugation detection method based on Gabor filtering, and Xiao et al. [66] proposed a technology that can detect the existence of defects and automatically classify them. This rail detection technology is based on the deformation texture analysis of the rail surface. In this method, a set of Gabor filters are used. The analysis of texture surfaces involves the recognition of texture attributes, which can be used for segmentation. What is more, Zhang et al. [67] adopted the variable step size LMS adaptive method to filter the collected response signals of the train axle box vibration acceleration sensor and then adopted parameter-optimization VMD and methods to process and analyze the filtered signals. The results show that this method can effectively decompose the vertical vibration acceleration signal of the axle box, calculate the envelope entropy of the decomposed signal, and obtain rail corrugation wavelength and position.

4.5. Other Methods

Generally, in addition to the aforementioned detection methods, many other research schemes are also investigated in this study. Gomes et al. [68] developed a software tool to analyze the railcar bogie accelerometer signal and quantify the track corrugation on the basis of its frequency and amplitude. The tool is compared with the power representation of a one-third octave filter used in industry. It was shown that the proposed tool can produce better results. Also, Bayesian methods can also be employed for rail-condition assessment [69–74]. Moreover, Xie et al. [75] presented an intelligent identification method of rail corrugation based on axle box acceleration based on a one-dimensional convolutional neural network (1-dcnn). A “spatial domain” cutting method is proposed to construct the appropriate 1-dcnn structure and configuration parameters, thus realizing the automatic extraction and classification of the input sample set data. In addition, the resolution of rail corrugation location and detection can be arbitrarily adjusted by setting the length of the “space window”. The results indicate that the proposed 1-dcnn method can identify and locate rail corrugations effectively, quickly, and stably. What is more, Teng et al. [76] built a new measurement system, named the 2D-RCM system, by using two-dimensional laser displacement sensors, as shown in Figure 12. The system can completely cover ultra-

shortwave and shortwave waveforms in one sampling and obtain the original multi-point data along the laser line directly. Finally, the accurate restoration of the corrugated rail is completed through the data-splicing method. The experimental results demonstrate that it has high precision in measuring the wavebands of corrugation varied from 10 mm to 1 m. Figure 12 shows the schematics of the traditional rail-corrugation measurement method.

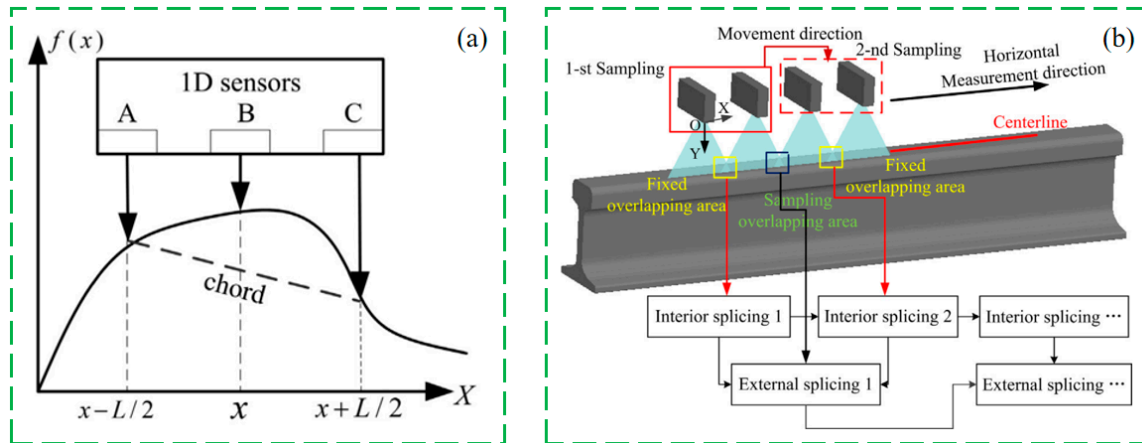


Figure 12. (a) Corrugation measurement means: chord-enabled method diagram; (b) 2D-RCM diagram [76].

In addition to the aforementioned studies, Sun et al. [77] used an independent energy collector to monitor railway wave grinding online. Through vibration tests, the corrugated defect of the rail is determined by using wavelet time-frequency analysis. It is concluded that the proposed method is able to collect the vibration energy of the track, and track corrugation can be identified by the induced voltage. The specific method is shown in the following Figure 13. Furthermore, Mei et al. [78] proposed a fast prediction method for rail corrugations, using SIMPACK to identify whether the creep force between wheel and rail is saturated according to the radius of the curved track. If the creep force is saturated, rail corrugation is considered to occur. The accuracy of this method can reach 85–90% or higher. Li et al. [79] developed a combination-chord model for data sharing. This model is used to measure rail corrugations from 30 mm to 60 m. It combines the advantages of the longwave corrugation measurement of the two-point string model and the shortwave corrugation measurement of the three-point asymmetric string model, and cleverly realizes the broadband waveform measurement of a three-point asymmetric string platform.

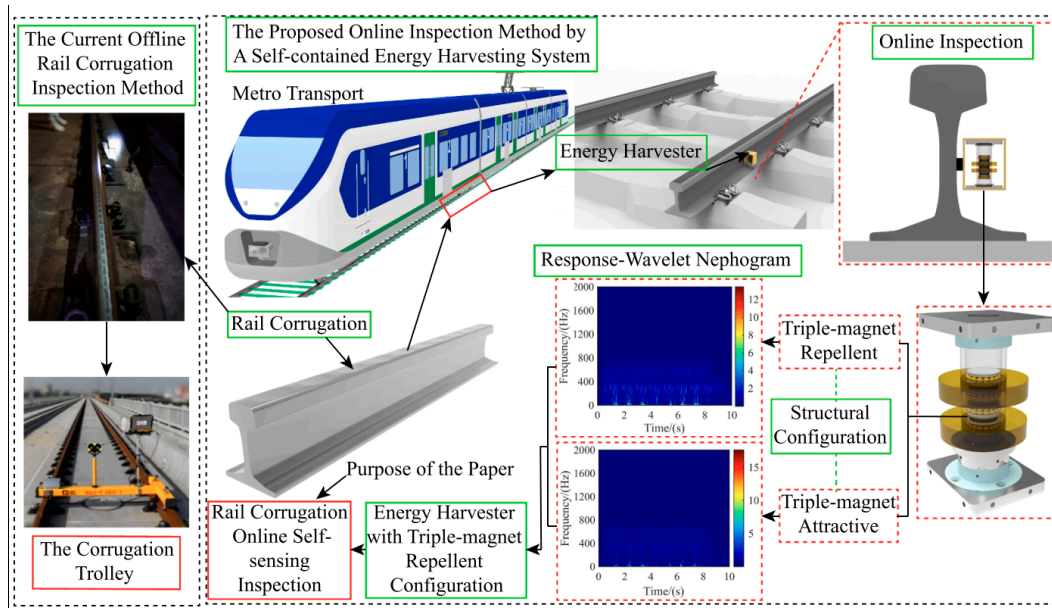


Figure 13. Configuration of online inspection method [77].

5. Concluding Remarks and Outlook

This study reviews a suite of the fundamental literature to demonstrate the recent developments in the study of rail corrugations. In this study, the definition and classification of rail corrugation are briefly introduced, with emphasis on the formation mechanism and detection method. On the basis of the extensive literature study, the following main conclusions can be drawn.

- (1) In summary, rail corrugations can be classified in three ways: corrugation classification by the wavelength, the wavelength determination mechanism, the rail damage mechanism, and the rail wear type;
- (2) The formation mechanism of rail corrugation includes wavelength-fixing theory and damage theory. According to the wavelength-fixing mechanism, the formation of corrugation is the result of the dynamic interaction between the wheel and the track. According to the damage mechanism, the corrugation is the plastic deformation of the track and the rolling contact fatigue wear;
- (3) The main adverse consequences caused by rail corrugations include damage to the train, damage to the track, rail component damage, and environmental radiation noise;
- (4) Detection methods of rail corrugations mainly include acceleration response, wavelet analysis, computer vision, digital filtering, etc. Acceleration measurement methods include techniques using fiber laser accelerometers and EEDM-based methods. The wavelet transform method uses wavelet packet energy entropy and a multi-body dynamics model to judge rail-corrugation conditions. The computer-vision-based method uses support-vector machines and classifiers to analyze railway images. The digital filtering algorithm includes a fast rail corrugation-detection method and Gabor filter technology.

Rail corrugation is a complicated problem with various formation mechanisms and abundant detection methods. However, there are still some limitations in this study, including the low detection efficiency and the inability to fully understand the long-term development trend of rail corrugations. Thus, the following future research should be carried out.

- (1) There still exists a high need to develop a more advanced corrugation-detection technology to improve detection accuracy and efficiency, as well as reduce maintenance costs;

- (2) On the basis of big data and machine-learning techniques, predictive models for rail corrugation development need to be built to identify and prevent corrugation problems in advance;
- (3) The environmental impact of rail corrugation, including noises and vibrations, should be further investigated to comprehensively assess its potential impact on the surrounding environment and society;
- (4) The scope of field monitoring should be expanded, and the observation period should be extended to obtain more realistic and comprehensive rail-corrugation data and provide a more reliable basis for the study of long-term corrugation-development trends.

Author Contributions: Conceptualization, Q.-A.W.; validation, X.-Y.H.; investigation, Q.-A.W.; resources, Y.-Q.N., S.-C.R., J.-P.L. and J.Z.; writing—original draft preparation, Q.-A.W. and X.-Y.H.; writing—review and editing, Q.-A.W., X.-Y.H., J.-F.W., S.-C.R., J.-P.L. and J.Z.; supervision, Q.-A.W.; funding acquisition, Q.-A.W., J.-F.W. and Y.-Q.N. All authors have read and agreed to the published version of the manuscript.

Funding: The study was supported by the National Key Research and Development Program of China under Award Number 2019YFE0118500, China Postdoctoral Science Foundation (2019M652006), a grant from the Research Grants Council of the Hong Kong Special Administrative Region (SAR), China (Grant No. R5020-18) and a grant from the Innovation and Technology Commission of the Hong Kong SAR Government (Grant No. K-BBY1). Shenzhen Science and Technology Program (Grant No. KQTD20180412181337494), Shenzhen Key Laboratory of Structure Safety and Health Monitoring of Marine Infrastructures (Grant No. ZDSYS20201020162400001).

Data Availability Statement: Not applicable.

Acknowledgments: The authors wish to express their gratitude to the staff and students in the Structural Engineering Laboratory for their extensive assistance.

Conflicts of Interest: The authors declare no conflict of interest.

References

1. Singh, P.; Elmi, Z.; Meriga, V.K.; Pasha, J.; Dulebenets, M.A. Internet of things for sustainable railway transportation: Past, present, and future. *Clean. Logist. Supply Chain* **2022**, *4*, 100065. [\[CrossRef\]](#)
2. Singh, P.; Pasha, J.; Moses, R.; Sobanjo, J.; Ozguven, E.E.; Dulebenets, M.A. Development of exact and heuristic optimization methods for safety improvement projects at level crossings under conflicting objectives. *Reliab. Eng. Syst. Saf.* **2022**, *220*, 108296. [\[CrossRef\]](#)
3. Singh, P.; Dulebenets, M.A.; Pasha, J.; Gonzales, E.D.R.S.; Lau, Y.Y.; Kampmann, R. Deployment of autonomous trains in rail transportation: Current trends and existing challenges. *IEEE Access* **2021**, *9*, 91427–91461. [\[CrossRef\]](#)
4. Troch, F.; Meersman, H.; Sys, C.; Van de Voorde, E.; Vanelslender, T. The added value of rail freight transport in Belgium. *Res. Transp. Bus. Manag.* **2022**, *44*, 100625. [\[CrossRef\]](#)
5. Karolina, K.P.; Marek, P.; Anna, O.K.; Emilia, K. Maritime or rail: Which of these will save the planet? EU Macro-Regional Strategies and Reality. *Sustainability* **2022**, *14*, 3555. [\[CrossRef\]](#)
6. Sato, Y.; Matsumoto, A.; Knothe, K. Review on rail corrugation studies. *Wear* **2002**, *253*, 130–139. [\[CrossRef\]](#)
7. Oostermeijer, K.H. Review on short pitch rail corrugation studies. *Wear* **2008**, *265*, 1231–1237. [\[CrossRef\]](#)
8. Ahlbeck, D.R.; Daniels, L.E. A review of rail corrugation processes under different operating modes. In Proceedings of the ASME/IEEE Joint Conference on Railroads, Chicago, IL, USA, 17–19 April 1990; pp. 13–17.
9. Grassie, S.L.; Kalousek, J. Rail corrugation: Characteristics, causes and treatments. *Proc. Inst. Mech. Eng. Part F J. Rail Rapid Transit* **1993**, *207*, 57–68. [\[CrossRef\]](#)
10. Nielsen, J.C.; Lunden, R.; Johansson, A.; Vernersson, T. Train-track interaction and mechanisms of irregular wear on wheel and rail surfaces. *Veh. Syst. Dyn.* **2003**, *40*, 3–54. [\[CrossRef\]](#)
11. Grassie, S.L. Rail corrugation: Advances in measurement, understanding and treatment. *Wear* **2005**, *258*, 1224–1234. [\[CrossRef\]](#)
12. Grassie, S.L. Rail corrugation: Characteristics, causes, and treatments. *Proc. Inst. Mech. Eng. Part F J. Rail Rapid Transit* **2009**, *223*, 581–596. [\[CrossRef\]](#)
13. Jin, X.S.; Li, X.; Li, W.; Wen, Z.F. Review of rail corrugation progress. *J. Pf Southwest Jiaotong Univ.* **2016**, *51*, 264–273.
14. Liu, G.; Wang, Q.A.; Jiao, G.Y.; Dang, P.Y.; Nie, G.H.; Liu, Z.C.; Sun, J.Y. Review of wireless RFID strain sensing technology in structural health monitoring. *Sensors* **2023**, *23*, 6925. [\[CrossRef\]](#) [\[PubMed\]](#)
15. Wang, Q.A.; Zhang, C.; Ma, Z.G.; Jiao, G.Y.; Jiang, X.W.; Ni, Y.Q.; Wang, Y.Q.; Du, Y.T.; Qu, G.B.; Huang, G.D. Towards long-transmission-distance and semi-active wireless strain sensing enabled by dual-interrogation-mode RFID technology. *Struct. Control Health Monit.* **2022**, *29*, e3069. [\[CrossRef\]](#)

16. Zarembski, A.M. Type of rail corrugation. *Rail Track Struct.* **1989**, *85*, 13.
17. Ahlback, D.R.; Daniels, L.E. Investigation of rail corrugation on the baltimore metro. *Wear* **1991**, *144*, 197–210. [[CrossRef](#)]
18. Matsumoto, A.; Sato, Y.; Ono, H.; Tanimoto, M.; Oka, Y.; Miyauchi, E. Formation mechanism and countermeasures of rail corrugation on curved track. *Wear* **2002**, *253*, 178–184. [[CrossRef](#)]
19. Liu, X.; Wang, P. Investigation of the generation mechanism of rail corrugation based on friction induced torsional vibration. *Wear* **2020**, *468–469*, 203593. [[CrossRef](#)]
20. Suda, Y.; Komine, H.; Iwasa, T.; Terumichi, Y. Experimental study on mechanism of rail corrugation using corrugation simulator. *Wear* **2002**, *253*, 162–171. [[CrossRef](#)]
21. Wang, Z.; Lei, Z. Analysis of influence factors of rail corrugation in small radius curve track. *Mech. Sci.* **2021**, *12*, 31–40. [[CrossRef](#)]
22. Wang, Z.; Lei, Z.; Zhu, J. Study on the formation mechanism of rail corrugation in small radius curves of metro. *J. Mech. Sci. Technol.* **2023**, *37*, 4521–4532. [[CrossRef](#)]
23. Du, X.; Jin, X.S.; Zhao, G.T.; Wen, Z.F.; Li, W. Rail corrugation of high-speed railway induced by rail grinding. *Shock. Vib.* **2021**, *2021*, 5546809. [[CrossRef](#)]
24. Meehan, P.; Batten, R.; Bellette, P. The effect of non-uniform train speed distribution on rail corrugation growth in cornering. *Wear* **2016**, *366–367*, 27–37. [[CrossRef](#)]
25. Cui, X.L.; Chen, G.X.; Yang, H.G.; Zhang, Q.; Ouyang, H.; Zhu, M.H. Effect of the wheel/rail contact angle and the direction of the saturated creep force on rail corrugation. *Wear* **2015**, *330–331*, 554–562. [[CrossRef](#)]
26. Chen, G.X.; Zhou, Z.R.; Ouyang, H.; Jin, X.S.; Zhu, M.H.; Liu, Q.Y. A finite element study on rail corrugation based on saturated creep force-induced self-excited vibration of a wheelset-track system. *J. Sound Vib.* **2010**, *329*, 4643–4655. [[CrossRef](#)]
27. Cui, X.L.; He, Z.Q.; Huang, B.; Chen, Y.C.; Du, Z.X.; Qi, W. Study on the effects of wheel-rail friction self-excited vibration and feedback vibration of corrugated irregularity on rail corrugation. *Wear* **2021**, *477*, 203854. [[CrossRef](#)]
28. Cui, X.L.; Chen, X.L.; Zhao, J.W.; Yan, W.Y.; Ouyang, H.; Zhu, M.H. Field investigation and numerical study of the rail corrugation caused by frictional self-excited vibration. *Wear* **2017**, *376*, 1919–1929. [[CrossRef](#)]
29. Ng, A.K.; Martua, L.; Sun, G. Influence of sleeper distance on rail corrugation growth. In Proceedings of the International Conference on Intelligent Rail Transportation (ICIRT), Singapore, 12–14 December 2018.
30. Ng, A.K.; Martua, L. Analysis and prediction of rail corrugation growth and axle box acceleration signals for different railway track configurations. In Proceedings of the 2021 7th International Conference on Control, Automation and Robotics (ICCAR), Singapore, 23–26 April 2021; pp. 275–279.
31. Vadillo, E.G.; Tarrago, J.; Zubiaurre, G.G.; Duque, C.A. Effect of sleeper distance on rail corrugation. *Wear* **1998**, *217*, 140–146. [[CrossRef](#)]
32. Meehan, P.A.; Bellette, P.A.; Batten, R.D.; Daniel, W.J.T.; Horwood, R.J. A case study of wear-type rail corrugation prediction and control using speed variation. *J. Sound Vib.* **2009**, *325*, 85–105. [[CrossRef](#)]
33. Cui, X.L.; He, Z.Q.; Huang, B.; Jiang, G. Study on the mechanism of the abnormal phenomenon of rail corrugation in the curve interval of a mountain city metro. *Tribol. Trans.* **2020**, *63*, 996–1007. [[CrossRef](#)]
34. Wu, Z.Z.; Wang, W.B.; Wang, X.S. Research on intelligent management of rail corrugation in urban rail transit. *Mod. Urban Rail Transit.* **2020**, *6*.
35. Li, J. Study on grinding treatment effect of wavy worn rail based on field test. *Railw. Constr. Technol.* **2019**, *44–49*.
36. Huang, W.Z.; Zhang, W.T.; Li, F. Detection of rail corrugation based on fiber laser accelerometers. *Meas. Sci. Technol.* **2013**, *24*, 094014. [[CrossRef](#)]
37. Li, J.B.; Shi, H.M. Rail corrugation detection of high-speed railway using wheel dynamic responses. *Shock. Vib.* **2019**, *2*, 2695647. [[CrossRef](#)]
38. Jiang, Z.Q.; Si, D.L.; Li, W. On rail corrugation of high-speed railway. *Chin. Railw. Sci.* **2014**, *35*, 9–14.
39. Molodova, M.; Li, Z.; Dollevoet, R. Axle box acceleration: Measurement and simulation for detection of short track defects. *Wear* **2011**, *271*, 349–356. [[CrossRef](#)]
40. Salvador, P.; Naranjo, V.; Insa, R.; Teixeira, P. Axlebox accelerations: Their acquisition and time-frequency characterisation for railway track monitoring purposes. *Measurement* **2016**, *82*, 301–312. [[CrossRef](#)]
41. Li, J.B.; Shi, H.M. Rail corrugation diagnosis of high-speed railway based on dynamic responses of the vehicle. In Proceedings of the Prognostics and Health Management Conference (PHM-Besançon), Besançon, France, 4–7 May 2020.
42. Wei, X.; Yin, X.; Hu, Y.; He, Y.; Jia, L. Squats and corrugation detection of railway track based on time-frequency analysis by using bogie acceleration measurements. *Veh. Syst. Dyn.* **2020**, *58*, 1167–1188. [[CrossRef](#)]
43. Wei, X.; Liu, F.; Jia, L. Urban rail track condition monitoring based on in-service vehicle acceleration measurements. *Measurement* **2016**, *80*, 217–228. [[CrossRef](#)]
44. Weston, P.F.; Ling, C.S.; Goodman, C.J.; Roberts, C.; Li, P.; Goodall, R.M. Monitoring lateral track irregularity from in-service railway vehicles. *Proc. Inst. Mech. Eng. Part F J. Rail Rapid Transit.* **2007**, *221*, 89–100. [[CrossRef](#)]
45. Wang, Y.; Qin, Y.; Wei, X. Track irregularities estimation based on acceleration measurements. In Proceedings of the International Conference on Measurement, Information and Control (MIC), Harbin, China, 18–20 May 2012; pp. 83–87.
46. Tanaka, H.; Matsumoto, M.; Harada, Y. Application of axle-box acceleration to track condition monitoring for rail corrugation management. In Proceedings of the 7th IET Conference on Railway Condition Monitoring 2016 (RCM 2016), Birmingham, UK, 27–28 September 2016; pp. 1–7.

47. Alten, K.; Fuchs, A. Detecting and classifying rail corrugation based on axle bearing vibration. In Proceedings of the IEEE International Conference on Acoustics, Speech and Signal Processing-Proceedings, Brighton, UK, 12–17 May 2019.
48. Grassie, S.; Kalousek, J. Rail ripple detection and classified vibration based on shaft bearing. *Proc. Inst. Mech. Eng. Part F J. Rail Rapid Transit.* **2017**, *207*, 57–68. [\[CrossRef\]](#)
49. Belov, I.V.; Shalymov, R.V.; Tkachenko, A.N.; Larionov, D.Y.; Podgornaya, L.N. Development of an algorithm for detecting railway corrugations in acceleration data. In Proceedings of the IEEE Conference of Russian Young Researchers in Electrical and Electronic Engineering, Moscow, Russia, 26–29 January 2021.
50. Dong, W.; Huang, W.; Xing, Z.Y. A rail corrugation detection method based on wavelet packet-energy entropy. *Railw. Stand. Des.* **2018**, *62*, 52–58.
51. Tsunashima, H.; Asano, A.; Ogino, M.; Asano, A. Condition monitoring of railway tracks using compact size on-board monitoring device. In Proceedings of the 6th IET Conference on Railway Condition Monitoring (RCM 2014), Birmingham, UK, 17–18 September 2014; pp. 1–5.
52. Cao, X.N.; Chai, X.D.; Zheng, S.B. Analysis of acceleration of train axle box based on hilbert-huang transformation. *Instrum. Tech. Sens.* **2015**, *3*, 92–95.
53. Kurzeck, B. Combined friction induced oscillations of wheelset and track during the curving of metros and their influence on corrugation. *Wear* **2011**, *271*, 299–310. [\[CrossRef\]](#)
54. Liu, X.J.; Han, J.; Xu, H.W.; Xiao, X.B.; Wen, Z.F.; Liang, S.L. An indirect method for rail corrugation measurement based on numerical models and wavelet packet decomposition. *Measurement* **2022**, *191*, 110726. [\[CrossRef\]](#)
55. Taheri, S.; Moslehi, B.; Sotoudeh, V.; Hopkins, B.M. Rail defect detection using fiber optic sensors and wavelet algorithms. In Proceedings of the ASME Joint Rail Conference, Pittsburgh, PA, USA, 18–20 April 2018.
56. Taheri, S.; Taheri, S. Rail track defect detection using derivative wavelet transform. In Proceedings of the Asme Rail Transportation Division Fall Conference, Omaha, NE, USA, 16–18 October 2012; pp. 51–56.
57. Li, Q.Y.; Tan, Y.G.; Zhang, H.Y.; Ren, S.W.; Dai, P.; Li, W.Y. A visual inspection system for rail corrugation based on local frequency features. 14th Intl Conf on Dependable, Autonomic and Secure Computing. In Proceedings of the 14th Intl Conf on Pervasive Intelligence and Computing, 2nd Intl Conf on Big Data Intelligence and Computing and Cyber Science and Technology Congress (DASC/PiCom/DataCom/CyberSciTech), Auckland, New Zealand, 8–12 August 2016.
58. Li, Q.Y.; Zhang, H.Y.; Ren, S.W.; Dai, P.; Li, W.Y. Detection method for rail corrugation based on rail image feature in frequency domain. *Zhongguo Tiedao Kexue/Chin. Railw. Sci.* **2016**, *37*, 24–30.
59. Li, Q.Y.; Shi, Z.P.; Zhang, H.Y.; Tan, Y.Q.; Ren, S.W.; Dai, P.; Li, W.Y. A cyber-enabled visual inspection system for rail corrugation. *Future Gener. Comput. Syst. FGCS* **2018**, *9*, 374–382. [\[CrossRef\]](#)
60. Wei, D.H.; Wei, X.K.; Liu, Y.X.; Jia, L.; Zhang, W.Q. The identification and assessment of rail corrugation based on computer vision. *Appl. Sci.* **2019**, *9*, 3913. [\[CrossRef\]](#)
61. Chen, L.; Li, Y.; Ma, Z.; Liu, H.; Mao, W. Vision-based position deviation measurement of rail corrugation chord measuring points under bi-linear laser assistance. *IEEE Access* **2021**, *9*, 36207–36217. [\[CrossRef\]](#)
62. Wang, C.; Zeng, J. Combination-chord measurement of rail corrugation using triple-line structured-light vision: Rectification and optimization. *IEEE Trans. Intell. Transp. Syst.* **2020**, *22*, 7256–7265. [\[CrossRef\]](#)
63. Mmg, S.; Younesian, D.; Torabi, M. A high accuracy and high-speed imaging and measurement system for rail corrugation inspection. *IEEE Trans. Ind. Electron.* **2020**, *68*, 8894–8903.
64. Yang, H.J.; Liu, J.X.; Mei, G.M.; Yang, D.S.; Deng, X.Q.; Duan, C. Research on real-time detection method of rail corrugation based on improved ShuffleNet V2. *Eng. Appl. Artif. Intell.* **2023**, *126*, 106825. [\[CrossRef\]](#)
65. Mandriota, C.; Nitti, M.; Ancona, N.; Stella, E.; Distanto, A. Filter-based feature selection for rail defect detection. *Mach. Vis. Appl.* **2004**, *15*, 179–185. [\[CrossRef\]](#)
66. Xiao, J.L.; Lu, K.X. Fast rail corrugation detection based on texture filtering. In Proceedings of the SPIE—The International Society for Optical Engineering, Xiangyang, China, 28–29 October 2017.
67. Zhang, H.Q.; Wang, N.; Liu, S.; Li, B.K. Track corrugation identification method based on parameter optimization VMD and spwvd. *Railw. Comput. Appl.* **2020**, *29*, 18–24.
68. Gomes, R.; Batista, A. Railscan: A tool for the detection and quantification of rail corrugation. In *FIP Advances in Information and Communication Technology*; Springer: Berlin/Heidelberg, Germany, 2010; Volume 314, pp. 401–408.
69. Wang, J.F.; Liu, X.Z.; Ni, Y.Q. A bayesian probabilistic approach for acoustic emission-based rail condition assessment. *Comput.-Aided Civ. Infrastruct. Eng.* **2018**, *33*, 21–34. [\[CrossRef\]](#)
70. Wang, Q.A.; Zhang, C.; Ma, Z.G.; Huang, J.D.; Ni, Y.Q.; Zhang, C. SHM deformation monitoring for high-speed rail track slabs and Bayesian change point detection for the measurements. *Constr. Build. Mater.* **2021**, *300*, 124337. [\[CrossRef\]](#)
71. Wang, Q.; Dai, Y.; Ma, Z.; Wang, J.; Lin, J.; Ni, Y.; Ren, W.; Jiang, J.; Yang, X.; Yan, J. Towards high-precision data modeling of SHM measurements using an improved sparse Bayesian learning scheme with strong generalization ability. *Struct. Health Monit.* **2024**, *23*, 588–604. [\[CrossRef\]](#)
72. Wang, Q.A.; Wu, Z. Structural system reliability analysis based on improved explicit connectivity BNs. *KSCE J. Civ. Eng.* **2018**, *22*, 916–927. [\[CrossRef\]](#)
73. Wang, Q.A.; Dai, Y.; Ma, Z.G.; Ni, Y.Q.; Tang, J.Q.; Xu, X.Q.; Wu, Z.Y. Towards probabilistic data-driven damage detection in SHM using sparse Bayesian learning scheme. *Struct. Control Health Monit.* **2022**, *29*, e3070. [\[CrossRef\]](#)

74. Wang, Q.A.; Wang, C.B.; Ma, Z.G.; Chen, W.; Ni, Y.Q.; Wang, C.F.; Yan, B.G.; Guan, P.X. Bayesian dynamic linear model framework for structural health monitoring data forecasting and missing data imputation during typhoon events. *Struct. Health Monit.* **2022**, *21*, 2933–2950. [[CrossRef](#)]
75. Xie, Q.L.; Tao, G.Q.; Wen, Z.F. Identification method of metro rail corrugation based on one-dimensional convolution neural network. *J. Cent. South Univ. (Nat. Sci. Ed.)* **2021**, *52*, 1371–1379.
76. Teng, Y.; Liu, H.L.; Liu, J.W.; Wang, C.; Ma, Z.J. A rail corrugation measurement method based on data splicing. *Measurement* **2020**, *156*, 107560. [[CrossRef](#)]
77. Sun, Y.H.; Wang, P.; Lu, J.; Xu, J.M.; Wang, P.G.; Xie, S.Y.; Li, Y.W.; Dai, J.; Wang, B.W.; Gao, M.Y. Rail corrugation inspection by a self-contained triple-repellent electromagnetic energy harvesting system. *Appl. Energy* **2021**, *286*, 116512. [[CrossRef](#)]
78. Mei, G.M.; Chen, G.X. Slip of wheels on rails: The root cause for rail undulant wear. *Wear* **2023**, *523*, 204727. [[CrossRef](#)]
79. Li, Y.F.; Liu, H.L.; Ma, Z.J.; Wang, C.; Zhong, X.Y. Rail corrugation broadband measurement based on combination-chord model and LS. *IEEE Trans. Instrum. Meas.* **2018**, *67*, 938–949. [[CrossRef](#)]

Disclaimer/Publisher’s Note: The statements, opinions and data contained in all publications are solely those of the individual author(s) and contributor(s) and not of MDPI and/or the editor(s). MDPI and/or the editor(s) disclaim responsibility for any injury to people or property resulting from any ideas, methods, instructions or products referred to in the content.